JOURNAL OF VIROLOGY, June 2005, p. 7721–7727 Vol. 79, No. 12
0022-538X/05/$08.00+0 doi:10.1128/JVI.79.12.7721–7727.2005

[^{18}F]FHPG Positron Emission Tomography for Detection of Herpes Simplex Virus (HSV) in Experimental HSV Encephalitis

A. R. Buursma,[1]* E. F. J. de Vries,[1] J. Garssen,[2] D. Kegler,[2] A. van Waarde,[1] J. Schirm,[3] G. A. P. Hospers,[4] N. H. Mulder,[4] W. Vaalburg,[1] and H. C. Klein[5]

PET Center, Groningen University Hospital, Groningen, The Netherlands[1]; Numico-Research, Wageningen, The Netherlands[2]; Laboratory for Infectious Diseases, Groningen, The Netherlands[3]; Department of Medical Oncology, Groningen University Hospital, Groningen, The Netherlands[4]; and Centre for Mental Health Winschoten, Winschoten, The Netherlands[5]

Received 18 November 2004/Accepted 18 February 2005

Herpes simplex virus type 1 (HSV-1) is one of the most common causes of sporadic encephalitis. The initial clinical course of HSV encephalitis (HSE) is highly variable, and the infection may be rapidly fatal. For effective treatment with antiviral medication, an early diagnosis of HSE is crucial. Subtle brain infections with HSV may be causally related to neuropsychiatric disorders such as Alzheimer's dementia. We investigated the feasibility of a noninvasive positron emission tomography (PET) imaging technique using [^{18}F]FHPG as a tracer for the detection of HSE. For this purpose, rats received HSV-1 (infected group) or phosphate-buffered saline (control group) by intranasal application, and dynamic PET scans were acquired. In addition, the distribution of tracer accumulation in specific brain areas was studied with phosphor storage imaging. The PET images revealed that the overall brain uptake of [^{18}F]FHPG was significantly higher for the infected group than for control animals. Phosphor storage images showed an enhanced accumulation of [^{18}F]FHPG in regions known to be affected after intranasal infection with HSV. High-performance liquid chromatography metabolite analysis showed phosphorylated metabolites of [^{18}F]FHPG in infected brains, proving that the increased [^{18}F]FHPG uptake in infected brains was due to HSV thymidine kinase-mediated trapping. Freeze lesion experiments showed that damage to the blood-brain barrier could in principle induce elevated [^{18}F]FHPG uptake, but this nonspecific tracer uptake could easily be discriminated from HSE-derived uptake by differences in the tracer kinetics. Our results show that [^{18}F]FHPG PET is a promising tool for the detection of HSV encephalitis.

Herpes simplex virus (HSV) is the most commonly recognized cause of acute sporadic encephalitis in humans in the Western world (19, 29, 33). Encephalitis is an acute and life-threatening infection of the brain parenchyma. If left untreated, HSV encephalitis (HSE) has an extremely high mortality rate of about 70%, with <3% of survivors regaining normal function. The exact incidence of HSE is not known, but it has been estimated to occur in approximately one to three individuals per million per year (19, 30). Approximately one-third of the patients that develop HSE are younger than 20 years of age, and 50% of the people who have HSE are older than 50 years of age (35).

Primary infection with HSV type 1 (HSV-1) usually occurs in the oropharyngeal mucosa. The primary infection usually is asymptomatic but can cause gingivostomatitis, pharyngitis, or respiratory disease (18). After the primary infection, HSV-1 is transported by transneuronal spread along a division of the trigeminal nerve. The virus then establishes latency in the trigeminal ganglion. The reactivation of a latent ganglionic infection with replication of the virus usually leads to cold sores (19). Sporadic anterograde transport from the ganglion may cause viral encephalitis with infection in the temporal cortex and limbic system structures (19, 29). The reactivation of latent HSV-1 can occur spontaneously or following various stimulating events. A variety of factors, such as stress, UV light, hormones, surgery, and radiotherapy, may play a role in the reactivation process of herpes simplex virus (28). The clinical presentation of HSE includes headache, fever, confusion, an altered level of consciousness, and sometimes psychosis as early signs (19, 23, 36). In the research field of Alzheimer's dementia, there is growing evidence supporting the hypothesis that the disease is in some instances related to a subtle encephalitic response to HSV-1 in the brain (16). Elevated antibodies against HSV-1 predict attenuated memory deficits in patients with schizophrenia (10), potentially due to brain activation of HSV-1.

The diagnosis of HSE is usually established by a combination of clinical and investigative features. The gold standard for diagnosing HSE has been the isolation of HSV from brain tissue. However, because of the risk of complications of brain biopsy, this diagnostic approach has never gained wide acceptance (26). In clinical practice, brain biopsies have been replaced with examinations of the cerebrospinal fluid (CSF), electroencephalography (EEG), and magnetic resonance imaging (MRI) (19, 20, 29). At present, MRI is the imaging method of choice for HSE because it provides the most sensitive method for detecting early lesions. The MRI scan may, however, be normal early in the infection (19, 29). During the acute stage of HSE, EEG generally shows various abnormalities, but when the acute phase is over, the EEG can become normal. A meta-analysis revealed that the sensitivity of EEG for the diagnosis of HSE is 86% and 100% for adults and neonates, respectively. The EEG abnormalities, however, are

* Corresponding author. Mailing address: PET Center, Groningen University Hospital, P.O. Box 30.001, 9700 RB Groningen, The Netherlands. Phone: 31-50-3613311. Fax: 31-50-3611687. E-mail: a.r.buursma@pet.azg.nl.

not specific to HSE, and thus, a confirmation of HSE by other methods is required (21). A CSF examination generally demonstrates elevations in protein concentrations and lymphocytic pleocytosis. Red blood cells are frequently (84%) seen as well. However, these changes are not specific to HSE, and normal CSF findings can appear during early disease. CSF viral cultures for HSV-1 are negative in >95% of cases. Elevated levels of antibodies to HSV are not seen in the CSF until 10 days to 2 weeks after the onset of disease (22).

The application of PCR to detect HSV DNA in the CSF has made a substantial contribution to the diagnosis of HSE. HSV PCR is a very sensitive method for the diagnosis of HSE, but the test may be negative during the first 24 to 48 h and after 10 days of symptoms (19, 29).

The drug of choice for the treatment of HSE is the nucleoside analogue acyclovir (ACV). ACV selectively inhibits the HSV-specific DNA polymerase and is activated specifically in HSV-infected cells, which express the HSV thymidine kinase (HSVtk) enzyme. The standard dose of ACV is 10 mg/kg of body weight three times daily for 14 days (19). For the successful treatment of HSE, therapy with ACV should be initiated early, as soon as the diagnosis of HSE is suspected (34). An early and accurate diagnosis of HSE is critical for the successful management of HSE.

We aim to develop a noninvasive tool to detect HSV encephalitis by using positron emission tomography (PET) imaging. For this purpose, we investigated the feasibility of using 9-[(1-[^{18}F]fluoro-3-hydroxy-2-propoxy)methyl]guanine ([^{18}F]FHPG) as the virus tracer. [^{18}F]FHPG is a derivative of ganciclovir, in which one hydroxyl group is replaced with a radioactive fluorine atom. [^{18}F]FHPG is selectively phosphorylated by the HSVtk enzyme. Phosphorylated [^{18}F]FHPG metabolites are selectively trapped within infected cells and can be monitored with PET. PET imaging with this tracer has proven to be successful for the detection of HSVtk-expressing C6 glioma cells outside the brain (14). Whether this tracer can also detect HSVtk in the HSV-infected brain is still unknown. For this study, we investigated the feasibility of the [^{18}F]FHPG PET technique for virus detection in an animal model of HSE. In this model, rats are inoculated intranasally with HSV-1. The virus has access to nervous tissue in a noninvasive manner via the olfactory pathway. Seven days after inoculation, viral replication is mainly observed in the brain, spinal cord, and ganglia (12). The viral spread in this model mimics an important route of viral infection for human HSE (11).

MATERIALS AND METHODS

Chemicals. Medetomidine (Domitor; 10 mg/ml) was obtained from Pfizer (New York, N.Y.), and ketamine (Ketanest; 25 mg/ml) was obtained from Parke-Davis (Munich, Germany).

Preparation of [^{18}F]FHPG. [^{18}F]FHPG was prepared as described by Alauddin et al. (1), with only minor modifications. The fluorination reaction was carried out at 125°C for 30 min and the subsequent hydrolysis was performed at 90°C for 5 min. The reaction mixture was neutralized by the addition of a sodium phosphate buffer (pH 7.2) prior to purification by high-performance liquid chromatography (HPLC), which was performed over a semipreparative Alltima C_{18} reverse-phase column (5 μm by 10 mm by 250 mm; Alltech, Deerfield, Ill.), with 3% ethanol–10 mM NaH_2PO_4 in saline as the eluent (flow rate, 5 ml/min; retention time, 16 min). The radiochemical yield was 5 to 15% (corrected for decay), and the radiochemical purity was >99% (HPLC was done with a Nova Pak C_{18} column [3 μm by 9 mm by 150 mm] with 2% acetonitrile; flow rate, 1 ml/min; retention time, 6 min).

Animal model. Male outbred WU (Wistar-Unilever) rats (6 to 8 weeks old) were obtained from the breeding colony of the National Institute for Public Health, Bilthoven, The Netherlands, or from Harlan, The Netherlands. The animals were housed separately in Macrolon cages and were provided with commercial rat chow (Hope Farms, Woerden, The Netherlands) and tap water ad libitum.

Infected group. Rats were infected intranasally with HSV-1. The HSV strain used for this study was a clinical isolate of a type 1 virus and was cultured in Vero cells and assayed for PFU per milliliter as described previously (12). Rats were anesthetized with ether and infected by the application of 100 μl of phosphate-buffered saline (PBS) containing 10^7 PFU of virus on the nostrils (50 μl per nostril). Sickness and behavior were scored daily.

Control group. Control animals were treated similarly, except that 100 μl of PBS without virus was applied (12).

Freeze lesion group. To investigate whether [^{18}F]FHPG PET could discriminate between HSV-1 infection and nonspecific damage to the blood-brain barrier, we performed freeze lesion experiments. Approximately 2 h before the PET study, rats were anesthetized with an intraperitoneal injection of a mixture of 25 mg/ml ketamine and 1 mg/ml medetomidine (5:1; 1 ml/kg). A skin flap was raised and a 5-mm trephination in the skull was made to expose the brain. Through the trephination, a freeze injury was produced by sequential 20- to 60-s applications of solid carbon dioxide powder (−81°C) to the dura overlying the right cerebral cortex (13). After the freeze lesion was produced, a 1-ml intravenous injection of Evans blue solution (2% in saline) was given to confirm the disruption of the blood-brain barrier.

All studies were carried out in compliance with the local ethical guidelines for animal experiments. The protocols were approved by the local animal ethics committee.

Viral load. For validation of our HSE model, HSV-1 titers in homogenized brains from infected animals were determined by a standard plaque assay, as previously described by Howie et al. (15). For groups of 20 rats each, the incidence of clinical symptoms was scored independent of the nature of the symptoms and correlated with the average viral load for the group.

PET studies. Seven days after inoculation of the rats with HSV-1 or PBS or 2 h after the application of a freeze lesion, dynamic PET scans were acquired. PET studies were performed by using a Siemens Exact HR+ positron camera (Siemens/CTI, Knoxville, Tenn.) with a resolution of about 5 mm (FWMH). Transmission and emission scans were obtained in the two-dimensional mode. The rats were anesthetized with an intraperitoneal injection of a mixture of 25 mg/ml ketamine and 1 mg/ml medetomidine (5:1; 1 ml/kg) and then were positioned in the PET camera with their long axis parallel to the transaxial plane of the tomograph in order to obtain sagittal sections. A transmission scan was obtained to correct for the attenuation of 511 keV of photons by tissue. An $H_2{}^{15}O$ PET scan was performed for anatomical localization of the brain. At least 15 min after the $H_2{}^{15}O$ PET data acquisition was completed, 18.8 ± 14.2 MBq of [^{18}F]FHPG was injected into the tail vein. Data were acquired for 1 h. Data analysis was performed with Siemens ECAT 7.1 software. In the images of the last frame of the $H_2{}^{15}O$ PET scan, regions of interest were drawn around the rat brain in the planes where the brain was clearly visible. These regions of interest were copied to the [^{18}F]FHPG emission images, and time-activity curves were calculated. Tracer accumulation is expressed as the percentage of the injected dose per gram of tissue (%ID/g). Statistical analysis was performed by using the two-sided unpaired Student t test. Significance was reached when the P value was <0.05.

After the PET scan, the rats were sacrificed by extirpation of the heart. The brain was either dissected and frozen in isopentane at −80°C for autoradiography purposes or dissected and homogenized for HPLC metabolite analysis and PCR analysis.

Autoradiography. The accumulation of [^{18}F]FHPG in specific brain areas was visualized by phosphor storage imaging. Frozen brain slices of 80-μm thickness were prepared with a Cryo-cut microtome (model 840; American Optical Corp., Buffalo, N.Y.) at −7°C. The slices were placed on object glasses and dried at room temperature. A Cyclone (multipurpose; Packard Instrument Company, Inc., Meriden, Conn.) storage phosphor screen was exposed to the brain slices for at least 36 h (20 half-lives of ^{18}F). The phosphor screen was analyzed with Optiquant analysis software (version 03.00; Packard Instrument Company, Inc., Meriden, Conn.). A calibration line was made during each experiment to convert the digital light units of the exposed screen into becquerels.

Regions of interest were drawn bilaterally over the nuclei olfactorius, the motor cortex, the somatosensory cortex, and the substantia nigra. The radioactivity in each area was quantified with the aid of the calibration line and was corrected for the injected dose of [^{18}F]FHPG and the tissue volume. Tracer uptake is expressed as the percentage of the injected dose (ID) per volume (ml)

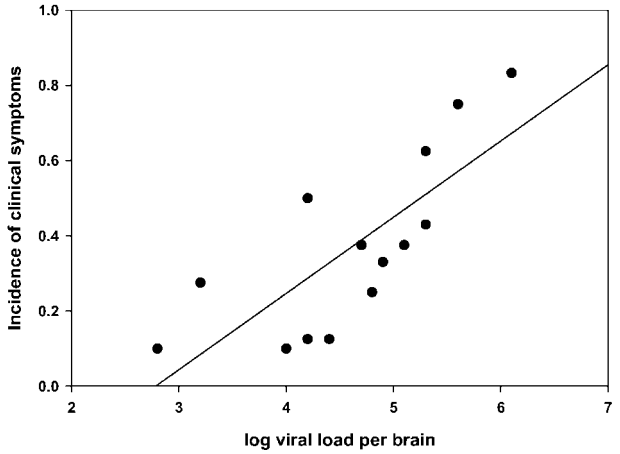

FIG. 1. Correlation between the incidence of clinical symptoms and the viral load in the brains of rats that were intranasally infected with HSV-1 7 days previously. Each dot in the graph represents the result for a group of 20 animals ($y = 0.20x - 0.57$; $r^2 = 0.59$; $P = 0.0013$).

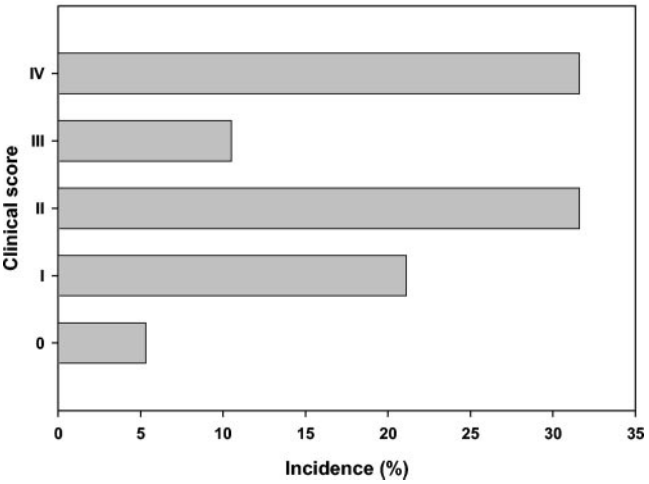

FIG. 2. Clinical symptoms in HSV-infected rats on day 7 after HSV-1 infection. The clinical symptoms were categorized and the percent incidence per category was calculated. 0, no symptoms; I, redness, swelling, and contamination of the nose and eyes; II, behavioral signs such as stress or lethargy; III, severe neurological signs such as impairment of motor function and paralysis; IV, death or termination.

of tissue. Statistical analysis was performed by using the two-sided unpaired Student *t* test. *P* values of <0.05 were considered significant.

Metabolite analysis. Metabolite analysis was performed by HPLC to determine the presence of phosphorylated [18F]FHPG metabolites. Brain tissue was homogenized in 1 ml of a 2% $HClO_4$ solution. The homogenate was centrifuged (3 min, 5,400 rpm), and the pellet was washed once with 1 ml and twice with 0.5 ml of 2% $HClO_4$. The radioactivity in the acid-soluble and acid-insoluble fractions was measured with a gamma counter. The acid-soluble fraction of the brain tissue was neutralized with 100 μg $NaHCO_3$, centrifuged (3 min, 5,400 rpm), and analyzed by reverse-phase HPLC (Alphabond C_{18} column [10 μm by 7.8 mm by 300 mm]; eluent, 4% ethanol; flow rate, 1.0 ml/min). The eluate was collected in fractions of 0.5 ml during a 45-min period and counted in a gamma counter. All radioactivity injected onto the HPLC column was recovered in the eluate.

HSV PCR. PCR analysis was performed with brain tissues from HSV-infected rats to confirm the presence of HSV-1. After the PET scan, a sample of the brain homogenate (as described above) was taken and DNAs were extracted from 100 μl of the homogenate by use of a MagnaPure total nucleic acid extraction kit. Real-time PCRs were performed with 5-μl DNA extracts in total volumes of 25 μl of universal master mix (Applied Biosystems), using TaqMan probes and the ABI Prism 7700 sequence detection system. A standard amplification protocol was used, consisting of 2 min at 50°C for the AmpErase uracil-*N*-glycosylase step, 10 min at 95°C for the activation of Ampli*Taq* Gold DNA polymerase, and 40 cycles of 15 s at 95°C and 1 min at 60°C. Type-common primers and probes selected from the gene coding for glycoprotein D were used for screening. When the HSV PCR was positive, the subtype was determined by real-time PCR using type-specific primers and probes, which reacted with a type-specific region of the gD gene (HSV-1) or the gG gene (HSV-2). The primers and probes were selected with Primer Express 2.0 and had the following sequences: HSV-1/2 primer 1, 5′-GCC GTC AGC GAG GAT AAC C; HSV-1/2 primer 2, 5′-GCT CGG TGC TCC AGG ATA AA; HSV-1/2 probe, 5′-FAM-CAC GTA CCT GCG GCT CGT GAA GAT AAA C-TAMRA; HSV-1 primer 1, 5′-TCC TSG TTC CTM ACK GCC TCCC; HSV-1 primer 2, 5′-GCA GIC AYA CGT AAC GCA CGC T; HSV-1 probe, 5′-FAM-CGT CTG GAC CAA CCG CCA CAC AGG T-TAMRA; HSV-2 primer 1, 5′-CGC CCA ATA CGC CTT AGC A; HSV-2 primer 2, 5′-GAG GTT CTT CCC GCG AAA T; and HSV-2 probe, 5′-FAM-CTC GCT TAA GAT GGC CGA TCC CAA TC-TAMRA.

RESULTS

Clinical symptoms. In groups of 20 rats each, the numbers of animals that showed any clinical symptom (irrespective of its nature) were scored until 7 days after infection. The incidence of clinical symptoms for each group correlated well with the average viral load in the brain (Fig. 1).

The first clinical signs of infection were seen on day 5 after HSV-1 infection. The severities of the clinical symptoms varied between individual animals and were categorized as follows: 0, no symptoms; I, redness, swelling, and contamination of the nose and eyes; II, behavioral signs such as stress or lethargy; III, severe neurological signs such as impairment of motor function and paralysis; and IV, death or termination due to ethical reasons. The incidences of these symptoms after HSV-1 infection are shown in Fig. 2. All animals in the control group appeared healthy. Scores for rats from other studies, which were treated similarly with the HSV-1 virus, were also included in the clinical scores.

All brain samples from HSV-1-infected rats tested positive by HSV-1 PCR and negative by HSV-2 PCR. These results confirmed that HSV disseminates to the brain after intranasal inoculation.

PET studies with HSV-1-infected and control rats. PET studies were performed with the HSV-1-infected group ($n = 8$) and the control group ($n = 3$). The PET images revealed that the overall brain uptake of [18F]FHPG was clearly elevated for the infected group. Average time-activity curves are shown in Fig. 3. In the control animals, the initial [18F]FHPG uptake was rapidly and completely washed out of the brain within 1 h. In the infected animals, the initial cerebral [18F]FHPG uptake was a little higher than that in control animals, and trapping of activity in the brain was observed. After 1 h, the average tracer uptake was $6.8 \times 10^{-2} \pm 3.2 \times 10^{-2}$ %ID/g for the infected group versus $0.36 \times 10^{-2} \pm 1.1 \times 10^{-2}$ %ID/g for the control group. The difference in tracer uptake in the brain between control rats and infected rats was statistically significant starting 17.5 min after tracer injection ($P < 0.05$).

An experimental observation that deserves separate attention is the fact that within the infected group, one animal did not show any clinical signs of infection (category 0). The tracer uptake in the brain of this animal was 0.83×10^{-2} %ID/g, as

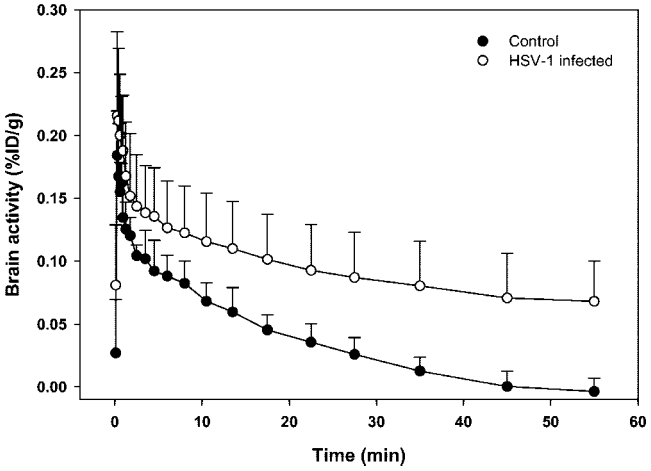

FIG. 3. Time-activity curves of [^{18}F]FHPG accumulation (%ID/g) in the brains of control rats and HSV-1-infected rats.

determined by PET, which was within the range of the tracer uptake in the brains of animals in the control group. The phosphor storage images of this animal showed only background activity levels, which were comparable to those of controls. All of the remaining infected rats with clinical symptoms of HSE showed uptakes of [^{18}F]FHPG above baseline levels.

Autoradiography. The resolution of our clinical PET camera did not allow us to discriminate between different areas in the brain. Therefore, the distributions of the virus in specific brain areas in the infected group and in the control group were studied by phosphor storage imaging. The phosphor storage images showed that [^{18}F]FHPG predominantly accumulated bilaterally in the nuclei olfactorius, the motor cortex, the somatosensory cortex, and the substantia nigra. In Fig. 4, the [^{18}F]FHPG uptake in these regions is shown in a phosphor image of a control rat brain and a rat brain with severe HSV infection. The average [^{18}F]FHPG uptake in each region is shown in Table 1 ($n = 6$ for the nuclei olfactorius and $n = 7$ for the remaining regions). These data represent the average [^{18}F]FHPG uptakes in the left and right hemispheres. In the infected brain, the [^{18}F]FHPG uptakes in the olfactorius, motor cortex, somatosensory cortex, and substantia nigra were

TABLE 1. [^{18}F]FHPG accumulation in some specified brain regions, as measured by phosphor storage imaging

Brain region	[^{18}F]FHPG accumulation (%ID/mL)[a]		*P* value
	HSV$^+$ group	Control group	
Olfactorius	0.0213 ± 0.0174	0.0067 ± 0.0006	0.068
Motor cortex	0.0168 ± 0.0103	0.0077 ± 0.0005	0.059
Somatosensory cortex	0.0146 ± 0.0080	0.0070 ± 0.0032	0.164
Substantia nigra	0.0137 ± 0.0056	0.0075 ± 0.0035	0.122

[a] Results are means ± standard deviations.

3.2, 2.2, 2.1, and 1.8 times higher, respectively, than those in the control brain. These differences in tracer uptake did not reach statistical significance because of the large variability in regional tracer uptake between individual animals in the infected group. This variability might be due to different migration routes of the virus through the brain, resulting in differences in the regional severity of infection between individual animals.

Metabolite analysis. To investigate whether [^{18}F]FHPG uptake in the brain was specifically due to HSV infection, we performed a metabolite analysis with infected brain tissue and control brain tissue. The acid-soluble fraction of the brain tissue was analyzed by reverse-phase HPLC at 1 h postinjection. In control brain tissue, >96% of the radioactivity in the acid-soluble fraction consisted of unmetabolized [^{18}F]FHPG. In HSV-infected brain tissue, approximately 15% polar metabolites were found (Fig. 5).

Freeze lesion experiments. To investigate whether [^{18}F]FHPG PET could discriminate between HSE and nonspecific damage to the blood-brain barrier, we performed freeze lesion experiments. Approximately 2 h after the application of a freeze lesion, dynamic PET scans were acquired. After 1 h, the tracer uptake was $4.0 \times 10^{-2} \pm 1.2 \times 10^{-2}$ %ID/g. Figure 6 shows a time-activity curve for the rats in the freeze lesion group ($n = 4$). For comparison, the time-activity curves for the infected and control groups are included. The curves were vertically translated until the maximum [^{18}F]FHPG activities were superimposed. From these normalized time-activity curves, differences in the tracer kinetics are obvious. After 1 h, the curve for the infected group reached a plateau, whereas the

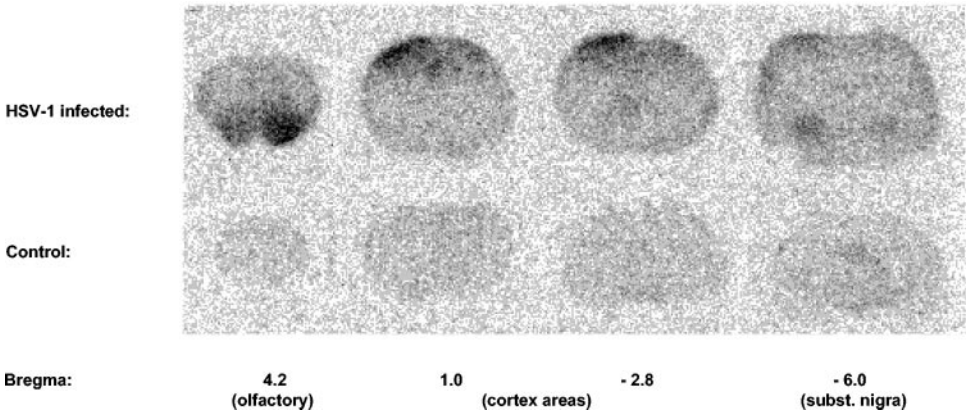

FIG. 4. Phosphor storage images of [^{18}F]FHPG uptake in control rat brain and rat brain with severe HSV-1 infection.

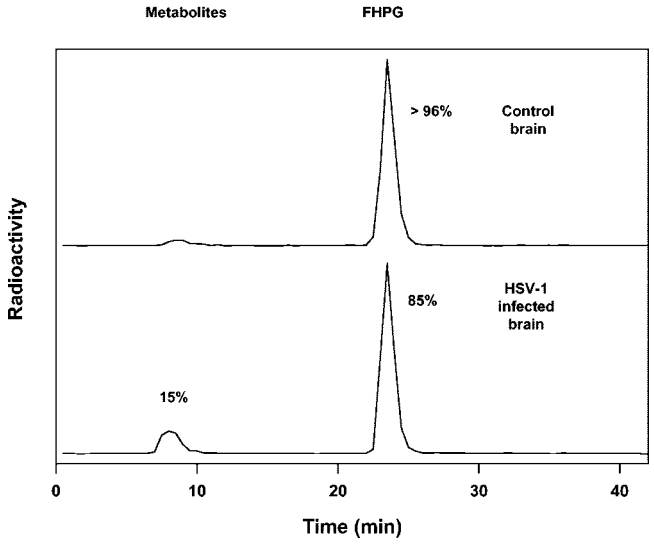

FIG. 5. [18F]FHPG metabolite analysis of acid-soluble fractions of HSV-1-infected brain tissue and control brain tissue by reversed-phase HPLC (60 min postinjection).

[18F]FHPG activities in the brains of animals in the freeze lesion and control groups still strongly decreased. The radioactivity was rapidly washed out for the freeze lesion group, and the decline in [18F]FHPG activity was comparable to that for the control group. However, the initial tracer uptake in the brains of animals with freeze lesions was higher than that for the control group. These results suggest that a freeze lesion leads to a high initial [18F]FHPG uptake caused by more perfusion of the brain tissue and that no trapping of radioactivity occurs.

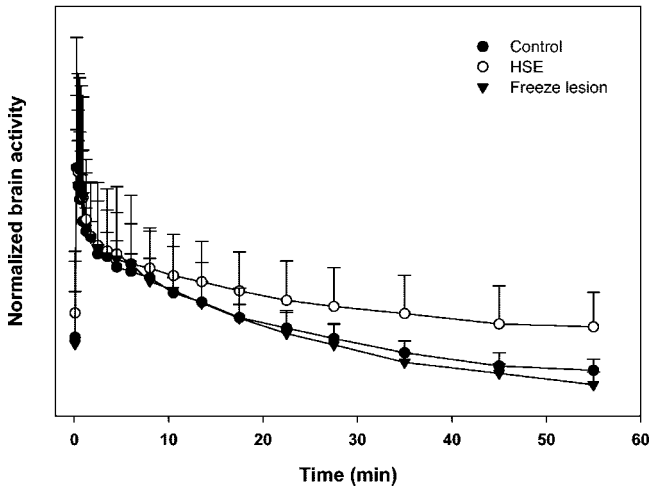

FIG. 6. Normalized time-activity curves of [18F]FHPG accumulation in the brains of rats in the freeze lesion group, rats in the infected group, and rats in the control group. The curves were vertically translated until maximum [18F]FHPG activities were superimposed.

DISCUSSION

The aim of this study was to explore whether [18F]FHPG PET could be a suitable method to detect HSV in the "encephalitic" brain. The HSV-encoded protein thymidine kinase (HSVtk) is one of the viral genomic elements that have been associated with neurovirulence (4). It plays an important role in HSV pathogenesis and appears to be necessary for reactivation from latency (8). A tk-deficient mutant of an HSV-1 strain caused decreased neurovirulence in a mouse model of HSV-1-induced encephalitis (7). tk mRNA transcription occurs at an early stage of HSV-1 infection: in explanted trigeminal ganglia removed from rabbits with previously established latency, the tk mRNA appeared in culture as early as 8 h after the start of incubation (27). Because of the aforementioned characteristics, HSVtk expression could be a target for imaging of HSE early after the onset of the disease. Previously, we have shown that HSVtk expression can be monitored in a double-tumor-bearing rat model by the use of [18F]FHPG PET (14). Whether [18F]FHPG PET can detect HSVtk inside the brain remained to be investigated. In a pharmacokinetic modeling study, the [18F]FHPG PET signal correlated well with the percentage of HSVtk-expressing cells (9). In addition, we reported that FHPG resembles ACV in its transport across the cell membrane and its phosphorylation characteristics (5). Therefore, we suggested that [18F]FHPG PET might be suitable for determining ACV's pharmacokinetics, which would allow for prediction of the treatment outcome for herpes-related diseases. This would be useful for HSE, which is treated with high doses of ACV.

For this study, the accumulation of [18F]FHPG was examined in the brains of intranasally HSV-infected rats. Previously, intranasal inoculation in a mouse model resulted in infection of brain regions that are also involved in the human disease, such as structures of the limbic system (31).

The present PET studies with [18F]FHPG showed an enhanced accumulation of the tracer in the brains of HSV-infected rats compared to brains of uninfected rats. Phosphor storage images showed that the accumulation of [18F]FHPG was enhanced in subregions known to be affected after intranasal infection with HSV, such as the olfactory nuclei (31).

The elevated [18F]FHPG uptake in the infected rats was supposed to be due to the trapping of [18F]FHPG metabolites within infected cells as a result of selective phosphorylation of the tracer by the HSVtk enzyme. This was confirmed by a metabolite analysis of HSV-infected brain tissue and control brain tissue. In control brain tissue, almost all radioactivity represented the parent compound. In HSV-infected brain tissue, not only unmetabolized FHPG but also phosphorylated metabolites were found, which accounted for approximately 15% of the radioactivity. To comprehend the large amount of unmetabolized [18F]FHPG in the infected brain homogenate, one should take into account that the majority of unmetabolized radioactivity in the brain was located in the blood compartment, whereas the metabolized fraction was located within brain cells. In a previous study, we demonstrated that all of the radioactivity in plasma consisted of an unmetabolized tracer (14). In addition, the phosphor storage imaging studies showed that the infection was restricted to specific small brain regions. In these regions, the elevated radioactivity represented the

metabolized and subsequently trapped [^{18}F]FHPG fraction. In uninfected regions, no metabolites will be formed. Fifteen percent phosphorylation in whole brain homogenates therefore seems relatively high, considering the fact that this percentage reflects only those small foci of infection.

During infection with HSV, swelling of the brain vasculature and tissue occurs. This suggests that during infection of the brain, the permeability of the blood-brain barrier may be altered (2). Furthermore, the release of chemical mediators such as bradykinin, arachidonic acid, histamine, and free radicals can cause an increase in the permeability of the blood-brain barrier (32). In previous biodistribution studies, we found that the uptake of [^{18}F]FHPG in brain tissue is approximately eightfold lower than the level of [^{18}F]FHPG in plasma (14). This low uptake of [^{18}F]FHPG in the brain reflects the restricted passage through the blood-brain barrier. In the case of HSV infection, damage to the blood-brain barrier and increased permeability could cause a leakage of [^{18}F]FHPG from the blood into the brain.

In order to investigate if damage to the blood-brain barrier itself could also induce a nonspecific elevation of [^{18}F]FHPG uptake in the brain, we performed freeze lesion experiments. A freezing injury to the cerebral cortex causes a disruption of the blood vessels at the site of the lesion, resulting in the movement of edema fluid from the damaged vessels into the extracellular space of the brain parenchyma (3).

The PET data for rats in the freeze lesion group showed an initial elevated [^{18}F]FHPG uptake compared to that of control rats. Apparently, the disruption of the blood-brain barrier at the site of the freeze lesion allows [^{18}F]FHPG to enter the brain. This was confirmed by brain phosphor storage images of rats in the freeze lesion group. The tracer uptake was elevated at the site of the freeze lesion only; there was no distribution of [^{18}F]FHPG to other brain regions. However, in contrast to the case for HSV-1-infected brains, the radioactivity in the brains of rats in the freeze lesion group was rapidly washed out. At 1 h postinjection, the radioactivity in the brain was still decreasing and no trapping of radioactivity occurred. In contrast, the cerebral [^{18}F]FHPG activity in the infected group reached a plateau and the majority of the radioactivity remained trapped in the brain, which reflected the trapping of phosphorylated FHPG metabolites. These differences in kinetics between the freeze lesion group and the infected group are illustrated in Fig. 6. The tracer kinetics in the brains of rats in the freeze lesion group were virtually the same as those for the control group. The freeze lesion experiments confirmed the fact that damage to the blood-brain barrier, which usually accompanies HSE, can initially cause a nonspecific elevation of [^{18}F]FHPG uptake in the brain by an improved perfusion of brain tissue. However, this nonspecific tracer uptake can be discriminated from HSE-derived uptake by the differences in tracer kinetics. Furthermore, with a freeze lesion, severe damage to the blood-brain barrier is accomplished. This is probably not comparable to the mild damage to the blood-brain barrier that can accompany HSE, and therefore our freeze lesion experiments do not represent ideal control experiments. However, even with this worst-case scenario, nonspecific [^{18}F]FHPG uptake could be discriminated from HSE-derived tracer uptake.

In this study, we examined whether encephalitis caused by HSV could be detected with [^{18}F]FHPG PET. Among the herpesviruses, HSV is the most frequent causal agent of encephalitis. In patients who are immunosuppressed, encephalitis may be caused by other herpesviruses as well, including varicella-zoster virus, Epstein-Barr virus, cytomegalovirus, and human herpesvirus 6 (29). All of these viruses encode a viral tk enzyme and are sensitive to acyclic guanosine-derived antiviral agents. It can be expected that [^{18}F]FHPG PET could be applied to detect other herpesviruses besides HSV. Infectious encephalitis is not only caused by herpesviruses but can also be due to infections by other viruses, bacteria, rickettsiae, fungi, or parasites (6). Rocky Mountain spotted fever, for example, is the most common rickettsial infection in the United States and may also cause encephalitis (29). Another example is the 1999 outbreak of encephalitis in New York, which was caused by West Nile virus (24). [^{18}F]FHPG PET should be able to discriminate herpesvirus-derived encephalitis from encephalitis caused by other infective agents. This is important information for determining the proper treatment strategy.

The observed phosphorylation of [^{18}F]FHPG provides "proof of principle" that FHPG accumulation is mediated by the intracellularly translated tk enzyme of HSV and demonstrates its diagnostic specificity for herpesvirus-derived encephalitis.

In addition, [^{18}F]FHPG PET might be suitable for determining ACV's pharmacokinetics, which could be applied to predict the efficacy of therapy with ACV, the drug of choice for treating HSE. Penetration within the cellular compartment and consecutive phosphorylation of ACV are prerequisites for the "viricidal" effect. The observation that [^{18}F]FHPG penetrates the living brain and is phosphorylated should predict the same stepwise accumulation of ACV and its effect against the infection. Whether [^{18}F]FHPG PET could discriminate between responders and nonresponders at the onset of treatment remains to be investigated.

There is increasing evidence of a potential viral cause of Alzheimer's dementia (17) and psychiatric disorders such as schizophrenia (25). For this hypothesis to be tested, a noninvasive technique to detect the virus is required. [^{18}F]FHPG PET could provide a tool to test the hypothesis that a herpesvirus is the cause of these devastating chronic diseases. Whether the technique is sufficiently sensitive to detect herpesvirus infections in the brains of human patients remains to be investigated.

We conclude that [^{18}F]FHPG PET appears suitable for monitoring intracellular herpesvirus infections in the living brain and may predict the efficacy of consecutive ACV therapy. [^{18}F]FHPG PET is a promising tool for the diagnosis and treatment evaluation of HSV encephalitis and, potentially, related neuropsychiatric disorders.

REFERENCES

1. **Alauddin, M. M., P. S. Conti, S. M. Mazza, F. M. Hamzeh, and J. R. Lever.** 1996. 9-[(3-[^{18}F]-fluoro-1-hydroxy-2-propoxy)methyl]guanine ([^{18}F]-FHPG): a potential imaging agent of viral infection and gene therapy using PET. Nucl. Med. Biol. **23:**787–792.
2. **Bidanset, D. J., L. Placidi, R. Rybak, J. Palmer, J. P. Sommadossi, and E. R. Kern.** 2001. Intravenous infusion of cereport increases uptake and efficacy of acyclovir in herpes simplex virus-infected rat brains. Antimicrob. Agents Chemother. **45:**2316–2323.
3. **Blasberg, R. G., J. Gazendam, C. S. Patlak, and J. D. Fenstermacher.** 1980. Quantitative autoradiographic studies of brain edema and a comparison of multi-isotope autoradiographic techniques. Adv. Neurol. **28:**255–270.
4. **Boivin, G., Z. Coulombe, and S. Rivest.** 2002. Intranasal herpes simplex virus

type 2 inoculation causes a profound thymidine kinase dependent cerebral inflammatory response in the mouse hindbrain. Eur. J. Neurosci. **16:**29–43.
5. **Buursma, A. R., I. J. van Dillen, A. van Waarde, W. Vaalburg, G. A. P. Hospers, N. H. Mulder, and E. F. J. de Vries.** 2004. Monitoring HSVtk suicide gene therapy: the role of [18F]FHPG membrane transport. Br. J. Cancer **91:**2079–2085.
6. **Chaudhuri, A., and P. G. Kennedy.** 2002. Diagnosis and treatment of viral encephalitis. Postgrad. Med. J. **78:**575–583.
7. **Chrisp, C. E., J. C. Sunstrum, D. R. Averill, Jr., M. Levine, and J. C. Glorioso.** 1989. Characterization of encephalitis in adult mice induced by intracerebral inoculation of herpes simplex virus type 1 (KOS) and comparison with mutants showing decreased virulence. Lab. Investig. **60:**822–830.
8. **Coen, D. M., M. Kosz-Vnenchak, J. G. Jacobson, D. A. Leib, C. L. Bogard, P. A. Schaffer, K. L. Tyler, and D. M. Knipe.** 1989. Thymidine kinase-negative herpes simplex virus mutants establish latency in mouse trigeminal ganglia but do not reactivate. Proc. Natl. Acad. Sci. USA **86:**4736–4740.
9. **de Vries, E. F. J., I. J. van Dillen, A. van Waarde, A. T. M. Willemsen, W. Vaalburg, N. H. Mulder, and G. A. P. Hospers.** 2003. Evaluation of [18F]F-HPG as PET tracer for HSVtk gene expression. Nucl. Med. Biol. **30:**651–660.
10. **Dickerson, F. B., J. J. Boronow, C. Stallings, A. E. Origoni, I. Ruslanova, and R. H. Yolken.** 2003. Association of serum antibodies to herpes simplex virus 1 with cognitive deficits in individuals with schizophrenia. Arch. Gen. Psychiatry **60:**466–472.
11. **Esiri, M. M.** 1982. Herpes simplex encephalitis. An immunohistological study of the distribution of viral antigen within the brain. J. Neurol. Sci. **54:**209–226.
12. **Garssen, J., R. van der Molen, A. de Klerk, M. Norval, and H. van Loveren.** 2000. Effects of UV irradiation on skin and nonskin-associated herpes simplex virus infections in rats. Photochem. Photobiol. **72:**645–651.
13. **Go, K. G., F. van Woudenberg, M. G. Woldring, E. J. Ebels, J. W. Beks, and E. H. Smeets.** 1969. The penetration of 14C-urea and 3H-water into the rat brain with cold-induced cerebral oedema. Histological and autoradiographic study of the oedema. The effect of urovert. Acta Neurochir. (Vienna) **21:**97–122.
14. **Hospers, G. A. P., A. Calogero, A. van Waarde, P. Doze, W. Vaalburg, N. H. Mulder, and E. F. J. de Vries.** 2000. Monitoring of herpes simplex virus thymidine kinase enzyme activity using positron emission tomography. Cancer Res. **60:**1488–1491.
15. **Howie, S. E. M., M. Norval, J. Maingay, and W. H. Mcbride.** 1986. Interactions between herpes-simplex virus and murine bone-marrow macrophages. Arch. Virol. **87:**229–239.
16. **Itzhaki, R. F., C. B. Dobson, and M. A. Wozniak.** 2004. Herpes simplex virus type 1 and Alzheimer's disease. Ann. Neurol. **55:**299–300.
17. **Itzhaki, R. F., M. A. Wozniak, D. M. Appelt, and B. J. Balin.** 2004. Infiltration of the brain by pathogens causes Alzheimer's disease. Neurobiol. Aging **25:**619–627.
18. **Johnson, R. T.** 1998. Viral infections of the nervous system. Lippincott-Raven, Philadelphia, Pa.
19. **Kennedy, P. G. E., and A. Chaudhuri.** 2002. Herpes simplex encephalitis. J. Neurol. Neurosurg. Psychiatry **73:**237–238.
20. **Kuker, W., T. Nagele, F. Schmidt, S. Heckl, and U. Herrlinger.** 2004. Diffusion-weighted MRI in herpes simplex encephalitis: a report of three cases. Neuroradiology **46:**122–125.
21. **Lai, C. W., and M. E. Gragasin.** 1988. Electroencephalography in herpes simplex encephalitis. J. Clin. Neurophysiol. **5:**87–103.
22. **Levitz, R. E.** 1998. Herpes simplex encephalitis: a review. Heart Lung **27:**209–212.
23. **Misra, P. C., and G. G. Hay.** 1971. Encephalitis presenting as acute schizophrenia. Br. Med. J. **1:**532–533.
24. **Nash, D., F. Mostashari, A. Fine, J. Miller, D. O'Leary, K. Murray, A. Huang, A. Rosenberg, A. Greenberg, M. Sherman, S. Wong, and M. Layton.** 2001. The outbreak of West Nile virus infection in the New York City area in 1999. N. Engl. J. Med. **344:**1807–1814.
25. **Pearce, B. D.** 2001. Schizophrenia and viral infection during neurodevelopment: a focus on mechanisms. Mol. Psychiatry **6:**634–646.
26. **Revello, M. G., and R. Manservigi.** 1996. Molecular diagnosis of herpes simplex encephalitis. Intervirology **39:**185–192.
27. **Rezuchova, I., M. Kudelova, V. Durmanova, A. Vojvodova, J. Kosovsky, and J. Rajcani.** 2003. Transcription at early stages of herpes simplex virus 1 infection and during reactivation. Intervirology **46:**25–34.
28. **Riel-Romero, R. M., and R. J. Baumann.** 2003. Herpes simplex encephalitis and radiotherapy. Pediatr. Neurol. **29:**69–71.
29. **Roos, K. L.** 1999. Encephalitis. Neurol. Clin. **17:**813–833.
30. **Skoldenberg, B.** 1996. Herpes simplex encephalitis. Scand. J. Infect. Dis. **100**(Suppl.)**:**8–13.
31. **Tomlinson, A. H., and M. M. Esiri.** 1983. Herpes simplex encephalitis. Immunohistological demonstration of spread of virus via olfactory pathways in mice. J. Neurol. Sci. **60:**473–484.
32. **Wahl, M., A. Unterberg, A. Baethmann, and L. Schilling.** 1988. Mediators of blood-brain barrier dysfunction and formation of vasogenic brain edema. J. Cereb. Blood Flow Metab. **8:**621–634.
33. **Whitley, R. J.** 1990. Viral encephalitis. N. Engl. J. Med. **323:**242–250.
34. **Whitley, R. J., C. A. Alford, M. S. Hirsch, R. T. Schooley, J. P. Luby, F. Y. Aoki, D. Hanley, A. J. Nahmias, and S. J. Soong.** 1986. Vidarabine versus acyclovir therapy in herpes simplex encephalitis. N. Engl. J. Med. **314:**144–149.
35. **Whitley, R. J., and D. W. Kimberlin.** 1999. Viral encephalitis. Pediatr. Rev. **20:**192–198.
36. **Wilson, L. G.** 1976. Viral encephalopathy mimicking functional psychosis. Am. J. Psychiatry **133:**165–170.